THE UNIVERSITY of TENNESSEE UT KNOXVILLE

Experimental and Computational Investigation of High-Entropy Alloys (HEAs) for Elevated-Temperature Applications

Investigators: Fan Zhang[2] and Peter K. Liaw[1]

Ph.D. Students: Haoyan Diao[1], Zhinan An[1], Haifei Li[1], Michael Hemphil[1], and Louis J. Santodonato[1, 3]

Collaborators: Chuan Zhang[2], Karin A. Dahmen[4], Jason S. C. Jang[5], Shizhong Yang[6], Michael Gao[7, 8], and Rajiv Mishra[9]

1. The University of Tennessee, Knoxville, TN 37996.
2. CompuTherm, LLC, Madison, WI 53719.
3. Oak Ridge National Laboratory, Oak Ridge, TN 37831.
4. The University of Illinois, Urbana, IL 61801.
5. National Centre University, Chung-Li, Taoyuan County, Taiwan, 32001.
6. Southern University and A&M College, Baton Rouge LA 70807.
7. National Energy Technology Laboratory, OR 97321.
8. URS Corporation, OR 97321-2198.
9. University of North Texas, TX 76203.

BIG ORANGE BIG IDEAS

1

THE UNIVERSITY of TENNESSEE UT KNOXVILLE

Acknowledgements

We are very grateful to:

- Vito Cedro
- Richard Dunst
- Patricia Rawls
- Robert Romanosky
- Susan Maley
- Conrad Regis
- Steven Markovich
- Nicholas Anderson for their kind support, and
- National Energy Technology Laboratory (NETL) for sponsoring this project

2

THE UNIVERSITY of TENNESSEE UT KNOXVILLE

Outline of Presentation

- Potential significance
- Background and unique behavior of HEAs
- Project objectives
- Proposed work
- Results and discussion
- Future work
- Published papers and presentations
- Conclusions

3

THE UNIVERSITY of TENNESSEE UT KNOXVILLE

Potential Significance

- Develop a suitable HEA for steam and gas turbine components operating at temperatures higher than 760° C.
- Increase the thermal efficiency of steam turbines and reduce the costs of fuel and emissions.
- Apply a computer-aided approach for designing new types of alloys applicable for the development of other high-temperature materials.

http://middleeast.geblogs.com/en/lang-en/ge-steam-turbines-to-help-saudi-arabia-boost-power-output-and-efficiency-2/

THE UNIVERSITY of TENNESSEE UT KNOXVILLE

Background and Unique Behavior

- Most alloy systems are based on a single principal element to form the matrix.
- Multiple principal elements were expected to yield many intermetallic compounds creating a complex microstructure.
- However, simple face-centered cubic (FCC) and body-centered cubic (BCC) structures are possible and thermodynamically favorable.

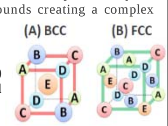

[1] J. W. Yeh, S. K. Chen, S. J. Lin, J. Y. Gan, T. S. Chin, T. T. Shun, C. H. Tsau, and S. Y. Chang, Advanced Engineering Materials 6, 299 (2004).
[2] B. Cantor, I. T. H. Chang, P. Knight, and A. J. B. Vincent, Materials Science and Engineering A 375-377, 213 (2004).
[3] Y. Zhang, T. T. Zuo, Z. Tang, M. C. Gao, K. A. Dahmen, P. K. Liaw, and Z. P. Lu, Progress in Materials Science 61, 1 (2014).

5

THE UNIVERSITY of TENNESSEE UT KNOXVILLE

Background and Unique Behavior (Cont'd)

- In equimolar ratios,

$$\Delta S_{conf} = k_B \cdot \ln(\Omega) = \frac{R}{N_A} \ln(N)^{N_A} = R \cdot \ln(N)$$

k: Boltzmann's constant
Ω: Number of ways of mixing
R: Gas Constant
N: Number of elements
N_A: Avogadro constant

High entropy of mixing and sluggish diffusion yield stable FCC and BCC solid solutions.

- Stable phases have the lowest Gibbs Free Energy

$$\Delta G = \Delta H - T\Delta S$$

G: Gibbs free energy
H: Enthalpy
T: Temperature
S: Entropy

At high temperatures, HEAs are stable and show great high-temperature strengths.

6

THE UNIVERSITY of TENNESSEE UT KNOXVILLE

Background and Unique Behavior (Cont'd)

Compression behavior at elevated temperatures

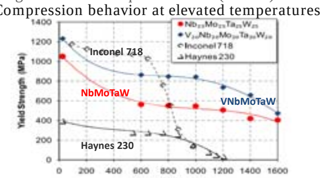

The yield stress of both alloys dropped by 30 - 40% between room temperature and 600 °C, but was relatively insensitive to temperature above 600 °C, comparing favorably with conventional superalloys.

O. N. Senkov, G. B. Wilks, J. M. Scott, and D. B. Miracle, Intermetallics 19, 698 (2011).
O. N. Senkov, G. B. Wilks, D. B. Miracle, C. P. Chuang, and P. K. Liaw, Intermetallics 18, 1758 (2010).

7

THE UNIVERSITY of TENNESSEE UT KNOXVILLE

Background and Unique Behavior (Cont'd)

Good Fatigue Resistance of Al0.5CoCrCuFeNi

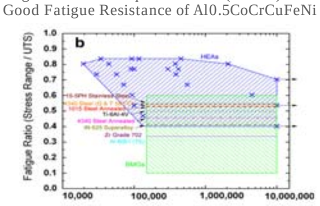

UTS: Ultimate Tensile Strength

M. A. Hemphill, T. Yuan, G. Y. Wang, J. W. Yeh, C. W. Tsai, A. Chuang, and P. K. Liaw, Acta Materialia 60, 5723 (2012).

8

THE UNIVERSITY of TENNESSEE UT KNOXVILLE

Background and Unique Behavior (Cont'd)

Good Fatigue Resistance of Al0.5CoCrCuFeNi

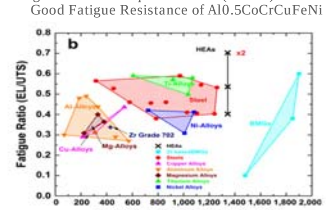

EL: Fatigue-Endurance Limit; UTS: Ultimate Tensile Strength

M. A. Hemphill, T. Yuan, G. Y. Wang, J. W. Yeh, C. W. Tsai, A. Chuang, and P. K. Liaw, Acta Materialia 60, 5723 (2012).

9

Project Objectives

- Perform fundamental studies on the $Al_xCrCuFeMnNi$ high-entropy alloy (HEA) system for use in boilers, and steam and gas turbines at temperatures above 760°C and a stress of 35 MPa.
- Develop the thermodynamic database and identify the potential HEAs within the Al-Cr-Cu-Fe-Mn-Ni system for further experimental investigation.
- Optimize microstructures to identify the best combined strength, ductility, and creep resistance.

Preliminary Results - Alloy Fabrication (Cont'd)

❖Al0.8CrCuFeMnNi (Al0.8CrCuFeMnNi-HIP-899°C)
❖Φ 25.4 mm (1 inch)✕ 762 mm (30 inch)
❖Vacuum Cast → Hot Isostatic Pressing (HIP) 899 °C, 103 MPa, 2 h.
❖Differential Thermal Analysis (DTA)
100 °C---1,600 °C

- No thermal transitions: 100 to around 980 °C.
- Three transitions occurred at 980 °C, 1,173 °C, and 1,358 °C.
- Discernible liquidus is not observed up to 1,600 °C.

Preliminary Results - Alloy Fabrication (Cont'd)

- For the same chemical composition, Al0.8CrCuFeMnNi, another specimen (Al0.8CrCuFeMnNi-as cast) was prepared by arc-melting elemental Al, Cr, Cu, Fe, Mn, and Ni raw materials in a water-cooled copper hearth. Its dimension is 100 mm × 80 mm × 10 mm.
- To study the aluminum effect, two new chemical compositions, Al0.1CrCuFeMnNi and Al0.3CrCuFeMnNi, are casted.

Microstructures (Al0.8CrCuFeMnNi-HIP-899°C)

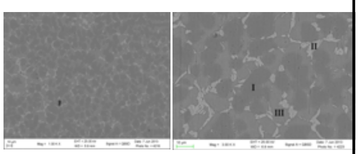

Atomic %	Al	Cr	Mn	Fe	Ni	Cu
Nominal	13.79	17.24	17.24	17.24	17.24	17.24
Dark-grey area (I)	8.12	31.88	15.47	29.04	9.05	6.44
White-phase layer (II)	6.97	1.65	19.12	3.11	9.90	59.25
Light-grey area (III)	20.97	4.86	19.31	6.59	28.13	20.14

Microstructures (Al0.8CrCuFeMnNi-as-cast)

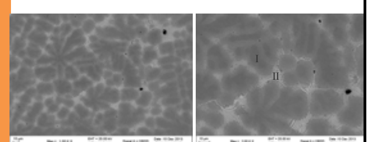

Atomic %	Al	Cr	Mn	Fe	Ni	Cu
Nominal	13.79	17.24	17.24	17.24	17.24	17.24
Dark-grey area (I)	14.84	10.97	17.91	26.71	17.67	11.90
White-phase layer (II)	13.18	1.4	21.13	6.35	15.37	42.57

Microstructures

Alloy Composition: $Al_{1.3}CoCrCuFeNi$

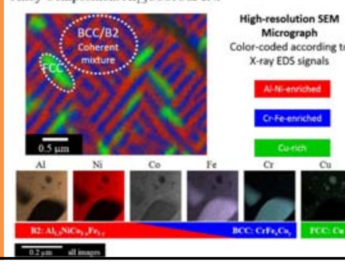

Microstructures

Atomic concentrations across the B2-FCC interface

Atom-probe tomography (APT)

Alloy composition: $Al_{1.3}CoCrCuFeNi$

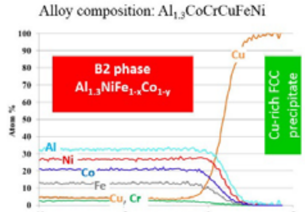

X-ray Diffraction Patterns

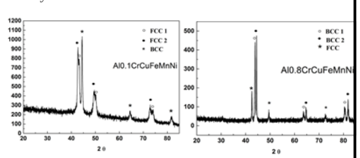

	FCC1	FCC2	BCC1	BCC2
Al0.1CrCuFeMnNi	▲	▲	▲	-
Al0.8CrCuFeMnNi	▲	-	▲	▲

In-situ neutron-diffraction experiments

Spallation Neutron Source (SNS), Oak Ridge National Laboratory (ORNL)

The Nanoscale-Ordered Materials Diffractometer (NOMAD)

- Al_xCoCrCuFeNi and Al_xMnCrCuFeNi specimens were heated all the way to the molten state using the newly-developed gas levitation and laser heating system

Aerodynamic Levitator

- Uses aerodynamic forces and CO_2 laser-beam heating
  - Greater than 2,500 °C achieved
- Containerless measurement
  - Avoids contamination
  - Avoids heterogeneous nucleation
  - Accesses supercooled liquids
  - Accesses clean liquid surfaces
- Beamline system for *in-situ* studies of structure in extreme conditions
- Developed through the DOE Small Business Innovation Research (SBIR) Grant
  - P.I. Dr. Richard Weber (Materials Development, Inc.)
  - SNS Collaborators, Dr. Joerg Neuefeind and Mr. Louis J. Santodonato

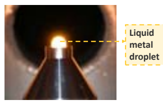

Above: Photo of a liquid metal droplet, levitated above a gas nozzle. **Below:** system schematic.

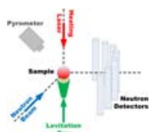

SNS NOMAD Beamline

Neutron Scattering Results

- Simple cubic structures
  - Face-centered-cubic (FCC)
  - Body-centered-cubic (BCC)
  - B2 (an ordered BCC variant)

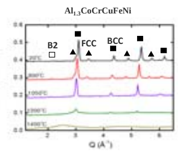

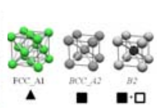

Results-Nanoindentation

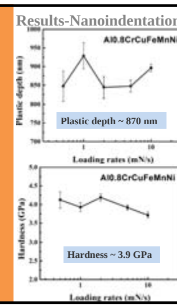

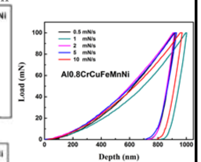

$$H = \frac{P_{max}}{A}$$

where P_{max} is the peak load, and A is the project contact area at the peak load.

21

Results-Nanoindentation

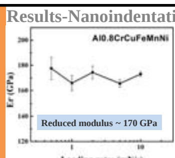

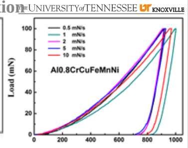

$$\frac{dP}{dh} = \frac{2}{\sqrt{\pi}} Er\sqrt{A}$$

dP/dh: the slope of the unloading load-displacement curve,
Er: the reduced modulus of a material
A: the projected contact area of the indent.

The reduced modulus of Al0.8CrCuFeMnNi is around 170 GPa, which is comparable to that of FeCoCrNiMn (179 ± 4 GPa).

P. Ternovskii, V. P. Alekhin, M. K. Shorshorov, M. M. Khrushchov, and V. N. Skvortsov. Zavodskaya Laboratoriya, 39, 1242(1974).
C. Zhu, Z. P. Lu, and T. G. Nieh, Acta Materialia, 2013, 61, 8 (2013).

22

Compression Tests

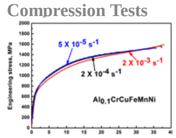

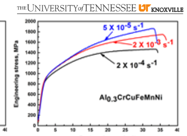

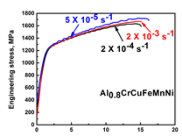

X = 0.1	X = 0.3
X = 0.8	

23

Compression Tests (Cont'd):

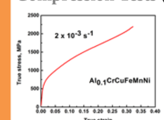

The relationship between true stress (strain) and engineering stress (strain)

$$\varepsilon_T = \ln(1+\varepsilon_E)$$
$$\sigma_T = \sigma_E(1+\varepsilon_E)$$

ε_T: true strain
ε_E: engineering strain
σ_T: true stress
σ_E: engineering stress

Strain Hardening

$$\sigma_T = K\varepsilon_T^n$$

K: constant
n: strain hardening exponent

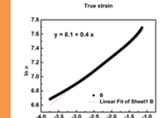

Al0.1CrCuFeMnNi
n = 0.41,
K = $e^{6.21}$ = 497 MPa

Callister, Jr., William D (2005), Fundamentals of Materials Science and Engineering (2nd ed.), pp: 152.

24

Compression Tests (Cont'd):

		2×10^{-3} s^{-1}	2×10^{-4} s^{-1}	5×10^{-5} s^{-1}
$Al_{0.1}CrCuFeMnNi$	n	0.41	0.37	0.36
	K (MPa)	498	567	584
$Al_{0.3}CrCuFeMnNi$	n	0.40	0.34	0.44
	K (MPa)	596	633	550
$Al_{0.8}CrCuFeMnNi$	n	0.23	0.22	0.24
	K (MPa)	1043	1054	1043

25

Compression Tests (Cont'd):

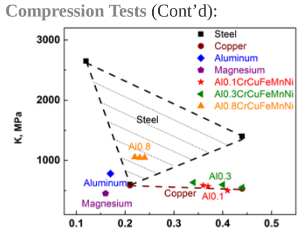

Callister, Jr., William D (2005), Fundamentals of Materials Science and Engineering (2nd ed.), pp: 152.

26

Compression Tests

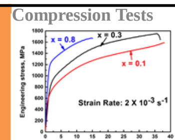

As the aluminum content increases,
- ❑ Yield stress increases
- ❑ Compression plasticity decreases

This phenomenon is due to the increased strengthening effect of lattice strains caused by the lattice-sites occupation of Al.

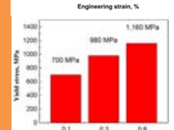

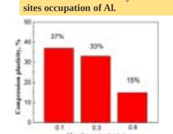

Z. Tang, M. C. Gao, H. Diao, T. Yang, J. Liu, T. Zuo, Y. Zhang, Z. Lu, Y. Cheng, Y. Zhang, K. A. Dahmen, P. K. Liaw, and T. Egami, JOM, 65, 12 (2013).

27

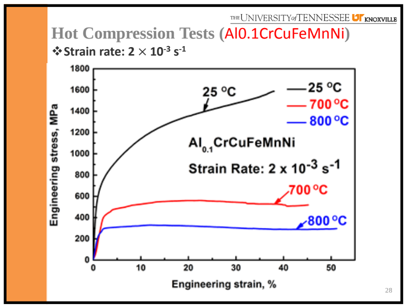
THE UNIVERSITY of TENNESSEE UT KNOXVILLE
Hot Compression Tests (Al0.1CrCuFeMnNi)
❖Strain rate: 2 × 10-3 s-1
25 °C
— 25 °C
— 700 °C
— 800 °C
Al0.1CrCuFeMnNi
Strain Rate: 2 x 10-3 s-1
700 °C
800 °C
Engineering stress, MPa
Engineering strain, %
28

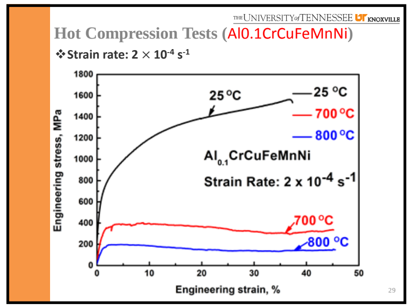
THE UNIVERSITY of TENNESSEE UT KNOXVILLE
Hot Compression Tests (Al0.1CrCuFeMnNi)
❖Strain rate: 2 × 10-4 s-1
25 °C
— 25 °C
— 700 °C
— 800 °C
Al0.1CrCuFeMnNi
Strain Rate: 2 x 10-4 s-1
700 °C
800 °C
Engineering stress, MPa
Engineering strain, %
29

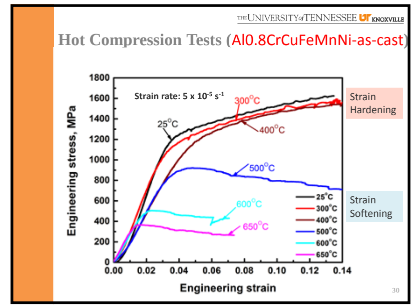
THE UNIVERSITY of TENNESSEE UT KNOXVILLE
Hot Compression Tests (Al0.8CrCuFeMnNi-as-cast)
Strain rate: 5 x 10-5 s-1
300°C
25°C
400°C
500°C
600°C
650°C
Strain Hardening
Strain Softening
25°C
300°C
400°C
500°C
600°C
650°C
Engineering stress, MPa
Engineering strain
30

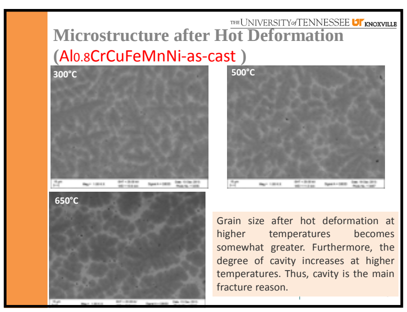
THE UNIVERSITY of TENNESSEE UT KNOXVILLE
Microstructure after Hot Deformation
(Al0.8CrCuFeMnNi-as-cast)
300°C
500°C
650°C
Grain size after hot deformation at higher temperatures becomes somewhat greater. Furthermore, the degree of cavity increases at higher temperatures. Thus, cavity is the main fracture reason.

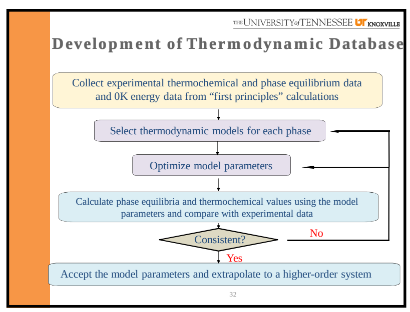
THE UNIVERSITY of TENNESSEE UT KNOXVILLE
Development of Thermodynamic Database
Collect experimental thermochemical and phase equilibrium data and 0K energy data from "first principles" calculations
Select thermodynamic models for each phase
Optimize model parameters
Calculate phase equilibria and thermochemical values using the model parameters and compare with experimental data
Consistent?
No
Yes
Accept the model parameters and extrapolate to a higher-order system
32

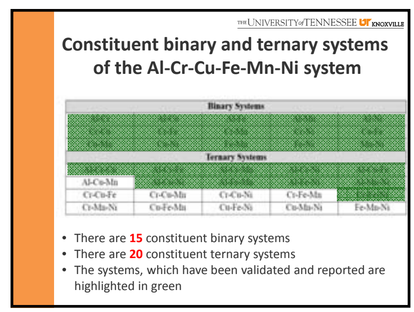
THE UNIVERSITY of TENNESSEE UT KNOXVILLE
Constituent binary and ternary systems of the Al-Cr-Cu-Fe-Mn-Ni system
Binary Systems
Ternary Systems
Al-Cu-Mn
Cr-Cu-Fe
Cr-Cu-Mn
Cr-Cu-Ni
Cr-Fe-Mn
Cr-Mn-Ni
Cu-Fe-Mn
Cu-Fe-Ni
Cu-Mn-Ni
Fe-Mn-Ni
• There are 15 constituent binary systems
• There are 20 constituent ternary systems
• The systems, which have been validated and reported are highlighted in green

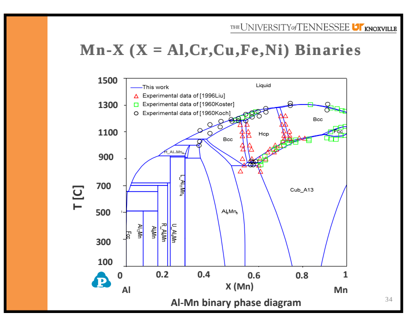
THE UNIVERSITY of TENNESSEE UT KNOXVILLE
Mn-X (X = Al,Cr,Cu,Fe,Ni) Binaries
This work
Experimental data of [1996Liu]
Experimental data of [1960Koster]
Experimental data of [1960Koch]
Liquid
Bcc
Hcp
Cub_A13
T [C]
X (Mn)
Al
Mn
Al-Mn binary phase diagram
34

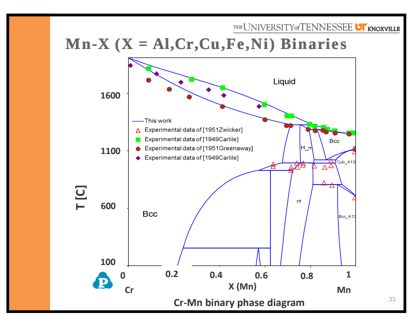
THE UNIVERSITY of TENNESSEE UT KNOXVILLE
Mn-X (X = Al,Cr,Cu,Fe,Ni) Binaries
Liquid
This work
Experimental data of [1951Zwicker]
Experimental data of [1949Carlile]
Experimental data of [1951Greenaway]
Experimental data of [1949Carlile]
Bcc
σ
T [C]
X (Mn)
Cr
Mn
Cr-Mn binary phase diagram
35

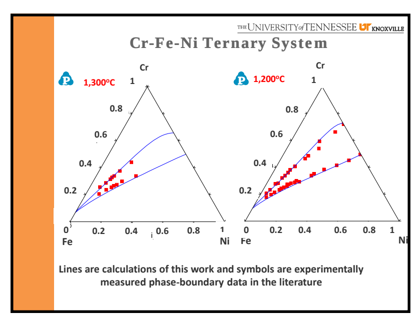
THE UNIVERSITY of TENNESSEE UT KNOXVILLE
Cr-Fe-Ni Ternary System
1,300°C
1,200°C
Cr
Fe
Ni
Lines are calculations of this work and symbols are experimentally measured phase-boundary data in the literature

THE UNIVERSITY of TENNESSEE UT KNOXVILLE

Cr-Fe-Ni Ternary System

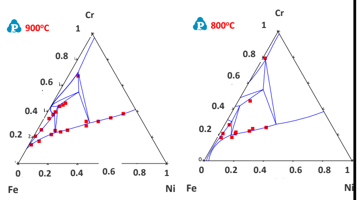

Lines are calculations of this work and symbols are experimentally measured phase-boundary data in the literature

THE UNIVERSITY of TENNESSEE UT KNOXVILLE

Future Work

- Fabricate high-quality HEA alloys
- Characterize the mechanical properties of the refined alloys
  - o Conduct nanoindentation experiments
  - o Perform compression tests
  - o Analyze and model in-situ neutron levitation results
  - o Carry out creep tests ex-situ as well as in-situ neutron diffraction
  - o Verify creep behavior by crystal-plasticity finite-element simulations.
- Study the performance of HEAs after aging
- Conduct experimental validation of the developed thermodynamic database based on the experimental data from both literature and our team members.

38

THE UNIVERSITY of TENNESSEE UT KNOXVILLE

Published Papers and Presentations

Papers:

[1] "Fatigue Behavior of Al0.5CoCrCuFeNi High Entropy Alloys", M. A. Hemphill, T. Yuan, G. Y. Wang, J. W. Yeh, C. W. Tsai, A. Chuang, and P. K. Liaw, Acta Materialia, Vol. 60, No. 16, pp. 5723-5734 (2012).

[2] "Microstructure and Compressive Properties of NbTiVTaAlx High Entropy Alloys", X. Yang, Y. Zhang, and P. K. Liaw, Procedia Engineering, Vol. 36, pp. 292-298 (2012).

[3] "Alloy Design and Properties Optimization of High-Entropy Alloys", Y. Zhang, X. Yang, and P. K. Liaw, JOM, Vol. 64, No. 7, pp. 830-838 (2012).

[4] "Processing and Properties of High-Entropy Alloys and Micro- and Nano-Wires", Y. Zhang, T. T. Zuo, W. B. Liao, and P. K. Liaw, ECS Transactions, Vol. 41, No. 30, pp. 49-60 (2012).

[5] "Local Atomic Structure of a High-Entropy Alloy: An X-Ray and Neutron Scattering Study", W. Guo, W. Dmowski, J. Y. Noh, P. Rack, P. K. Liaw, and T. Egami, Metallurgical and Materials Transactions a-Physical Metallurgy and Materials Science, Vol. 44A, No. 5, pp. 1994-1997 (2013).

[6] "Mechanical Properties of the High-Entropy Alloy Ag0.5CoCrCuFeNi at Temperatures of 4.2-300k", M. A. Laktionova, E. D. Tabchnikova, Z. Tang, and P. K. Liaw, Low Temperature Physics, Vol. 39, No. 7, pp. 630-632 (2013).

[7] "A Successful Synthesis of the Cocrfenial0.3 Single-Crystal, High-Entropy Alloy by Bridgman Solidification", S. G. Ma, S. F. Zhang, M. C. Gao, P. K. Liaw, and Y. Zhang, JOM, Vol. 65, No. 12, pp. 1751-1758 (2013).

39

Papers (Cont'd):

THE UNIVERSITY of TENNESSEE UT KNOXVILLE

[8] "A Tensile Deformation Model for in-Situ Dendrite/Metallic Glass Matrix Composites", J. W. Qiao, T. Zhang, F. Q. Yang, P. K. Liaw, S. Pauly, and B. S. Xu, Scientific Reports, Vol. 3, pp. 2816 (2013).

[9] "Aluminum Alloying Effects on Lattice Types, Microstructures, and Mechanical Behavior of High-Entropy Alloys Systems", Z. Tang, M. C. Gao, H. Diao, T. Yang, J. Liu, T. Zuo, Y. Zhang, Z. Lu, Y. Cheng, Y. Zhang, **K. A. Dahmen**, P. K. Liaw, and T. Egami, JOM, Vol. 65, No. 12, pp. 1848-1858 (2013).

[10] "Nature of the Interfaces between the Constituent Phases in the High Entropy Alloy Cocrcufenial", B. A. Welk, R. E. Williams, G. B. Viswanathan, M. A. Gibson, P. K. Liaw, and H. L. Fraser, Ultramicroscopy, Vol. 134, pp. 193-9 (2013).

[11] "High-Entropy Alloys with High Saturation Magnetization, Electrical Resistivity, and Malleability", Y. Zhang, T. T. Zuo, Y. Q. Cheng, and P. K. Liaw, Scientific Reports, Vol. 3, No., (2013).

[12] "Processing Effects on the Magnetic and Mechanical Properties of Feconial0.2si0.2 High Entropy Alloy", T. T. Zuo, S. B. Ren, P. K. Liaw, and Y. Zhang, International Journal of Minerals Metallurgy and Materials, Vol. 20, No. 6, pp. 549-555 (2013).

[13] "Microstructures and Crackling Noise of AlxNbTiMoV High Entropy Alloys", S. Chen, X. Yang, **K. Dahmen**, P. Liaw, and Y. Zhang, Entropy, Vol. 16, No. 2, pp. 870-884 (2014).

[14] "Symposium on High-Entropy Alloys Foreword", P. K. Liaw, G. Y. Wang, M. C. Gao, and S. N. Mathaudhu, Metallurgical and Materials Transactions a-Physical Metallurgy and Materials Science, Vol. 45A, No. 1, pp. 179-179 (2014).

40

Papers (Cont'd):

THE UNIVERSITY of TENNESSEE UT KNOXVILLE

[15] "Alloying and Processing Effects on the Aqueous Corrosion Behavior of High-Entropy Alloys", Z. Tang, L. Huang, W. He, and P. K. Liaw, Entropy, Vol. 16, No. 2, pp. 895-911 (2014).

[16] "Microstructures and Properties of High-Entropy Alloys", Y. Zhang, T. T. Zuo, Z. Tang, M. C. Gao, **K. A. Dahmen**, P. K. Liaw, and Z. P. Lu, Progress in Materials Science, Vol. 61, pp. 1-93 (2014).

[17] "Microstructures and Crackling Noise of AlxNbTiMoV High Entropy Alloys“, S. Y. Chen, X. Yang, **K. A. Dahmen**, P. K. Liaw, and Y. Zhang, Entropy, Vol. 16, pp. 870-884 (2014).

41

Presentation (Cont'd):

THE UNIVERSITY of TENNESSEE UT KNOXVILLE

- ❖ The 9th International Conference on Bulk Metallic Glass (BMG-IX) 2012, Xiamen, China
  - ▪ Computational Thermodynamics Aided High-Entropy Alloy Design, C. Zhang, F. Zhang, S. L. Chen, W. S. Cao, Z. Tang, P. K. Liaw
- ❖ 2013 TMS Meeting , San Antonio, TX, USA, March 3-9, 2013
  - ▪ Automatic Fabrication of High-Entropy Alloys and Their Properties, Y. Yokoyama, X. Xie, J. Antonaglia, M. Hemphill, T. Zhi, T. Yuan, G. Wang, C. Tsai, J. Yeh, A. Chuang, **K. Dahmen**, P. K. Liaw (invited)
  - ▪ Extracting Materials Properties from Crackling Noise and Slip Avalanche Statistics of Slowly-Sheared Materials, **K. Dahmen**, X. Xie, J. Antonaglia, M. Laktionova, E. Tabachnikova, Z. Tang, J. Qiao, J. Greer, J. W. Yeh, J. Uh, P. Liaw
  - ▪ Non-Equilibrium and Equilibrium Phases in AlCoCrFeNi High-Entropy Alloys, Z. Tang, O. Senkov, C. Parish, L. Santodonato, D. Miracle, G. Wang, C. Zhang, F. Zhang, P. K. Liaw
  - ▪ Ordering Behavior in the Al(x)CoCrCuFeNi High-Entropy Alloys, L. Santodonato, Y. Zhang, M. Gao, C. Parish, M. Feygenson, Z. Tang, J. Neuefeind, R. Weber, P. K. Liaw
  - ▪ Computational Modeling of High-Entropy Alloys, M. Gao, D. Tafen, J. Hawk, Y. Wang, M. Widom, L. Santodonato, P. K. Liaw(invited)

42

Presentation (Cont'd):

THE UNIVERSITY of TENNESSEE UT KNOXVILLE

- ▪ Minor Phase and Defect Effects on Fatigue Behavior of Wrought Al0.5CoCrCuFeNi High-Entropy Alloys, Z. Tang, M. Hemphill, T. Yuan, G. Wang, J. Yeh, C. Tsai, P. K. Liaw
- ▪ Phase Separation and Intermetallic Formation in "High-Entropy" Alloys, C. Parish, M. Miller, L. Santodonato, Z. Tang, P. K. Liaw.
- ▪ Computational Thermodynamics Aided High-Entropy Alloy Design, C. Zhang, F. Zhang, S. Chen, W. Cao, J. Zhu, Z. Tang, P. K. Liaw
- ▪ Statistical Fatigue-Life Modeling for High-Entropy Alloys, T. Yuan, M. Hemphill, Z. Tang, G. Wang, A. Chuang, C. Tsai, J. Yeh, P. K. Liaw (invited).
- ▪ A Combinatorial Approach to the Investigation of Metal Systems that Form Both High Entropy Alloys and Bulk Metallic Glasses, B. Welk, P. K. Liaw, M. Gibson, H. Fraser

- ❖ 2014 TMS Meeting, San Diego, CA, USA, February 16-20, 2014
  - ▪ Aluminum Alloying Effects on Lattice Types, Microstructures, and Mechanical Behavior of High-entropy Alloys Systems, Z.Tang, M. Gao, H. Y. Diao, T. F. Yang, J. P. Liu, T. T. Zuo, Y. Zhang, Z. P. Lu, Y. Q. Cheng, Y. W. Zhang, **K. Dahmen**, P. K. Liaw, T. Egami.
  - ▪ The Influence of Cu and Al on the Microstructure, Mechanical Properties and Deformation Mechanisms in the High Entropy Alloys CrCoNiFeCu, CrCoNiFeAl1.5 and CrCoNiFeCuAl1.5, B. Welk, B. B. Viswanathan, M. Gibson, P. K. Liaw, and H. Fraser.

43

THE UNIVERSITY of TENNESSEE UT KNOXVILLE

Presentation (Cont'd):

- ▪ The Influence of Alloy Composition on the Interrelationship between Microstructure Mechanical Properties of High Entropy Alloys with BCC/B2 Phase Mixtures, B. Welk, D. Huber, J. Jensen, G. Viswanathan, R. Williams, P. K. Liaw, M. Gibson, D. Evans, and H. Fraser.
- ▪ The Oxidation Behavior of AlCoCrFeNi High-entropy Alloy at 1023-1323K (750-1050oC), Wu Kai, W. S. Chen, C. C. Sung, Z. Tang, and P. K. Liaw.
- ▪ Strain-rate Effects on the Structure Evolution of High Entropy Alloys, X. Xie, J. Antonaglia, J. P. Liu, Z. Tang, J. W. Qiao, G. Y. Wang, Y. Zhang, K. Dahmen, and P. K. Liaw.
- ▪ Neutron diffraction studies on creep deformation behavior in a high-entropy alloy CoCrFeMnNi under high temperature and low strain rate, W. C. Woo, E. W. Huang, J. W. Yeh, P. K. Liaw, and H. Choo.
- ▪ The Hot Corrosion Resistance Properties of AlxFeCoCrNi, **S. Z. Yang**, M. Habibi, L. Wang, S. M. Guo, Z. Tang, P. K. Liaw, L. X. Tan, C. Guo, and M. Jackson.
- ▪ Using the Statistics of Serrations in the Stress Strain Curves to Extract Materials Properties of Slowly-sheared High Entropy Alloys, **Karin Dahmen**, X. Xie, J. Antonaglia, M. Laktionova, E. Tabachnikova, J. W. Qiao, J. W. Yeh, C. W. Tsai, J. Uh, and P. K. Liaw.

44

Presentation (Cont'd):

THE UNIVERSITY of TENNESSEE UT KNOXVILLE

- ▪ Environmental-temperature Effect on a Ductile High-entropy Alloy Investigated by In Situ Neutron-diffraction Measurements, E. W. Huang, C. Lee, D. J. Yu, K. An, P. K. Liaw, and J. W. Yeh.
- ▪ Mechanical Behavior of an Al0.1CoCrFeNi High Entropy Alloy, M. Komarasamy, N. Kumar, Z. Tang, **R. Mishra**, and P. K. Liaw.
- ▪ Characterizing Multi-component Solid Solutions Using Order Parameters and the Bragg-Williams Approximation, L. Santodonato, and P. K. Liaw.
- ▪ Ultra Grain Refinement in High Entropy Alloys, N. Tsuji, I. Watanabe, N. Park, D. Terada, A. Shibata, Y. Yokoyama, P. K. Liaw.
- ▪ Nanostructure Evolution through High-pressure Torsion and Recrystallization in a High-entropy CrMnFeCoNi Alloy, N. Park, A. Shibata, D. Terada, Y. Yokoyama, P. K. Liaw, and N. Tsuji.
- ▪ Distinguished Work-hardening Capacity of a Ti-based Metallic Glass Matrix Composite upon Dynamic Loading, J. W. Qiao, H. J. Yang, Z. H. Wang, and P. K. Liaw.

- ❖ The 10th International Conference on Bulk Metallic Glass 2014, Shanghai, China, University of Science and Technology, Beijing, June 6-16, 2014
  - ▪ Characterization of Serrated Flows in BMG and HEAs, X. Xie, S. Y. Chen, J. Auto, J. P. Liu, J. W. Qiao, P. K. Liaw (invited).
- ❖ National Institute of Materials Science, Japan, 2014
  - ▪ Fatigue Behavior of BMG and HEAs, X. Xie, G. Y. Wang, P. K. Liaw.

45

THE UNIVERSITY of TENNESSEE UT KNOXVILLE

Conclusions

- We have fabricated the Al0.1CrCuFeMnNi alloy, Al0.3CrCuFeMnNi alloy, and Al0.8CrCuFeMnNi alloys.
- The Al0.1CrCuFeMnNi alloy has three phases, FCC1, FCC2, and BCC. The Al0.8CrCuFeMnNi alloys have the structure, including three phases, disordered BCC1, BCC2, and FCC phases.

46

THE UNIVERSITY of TENNESSEE UT KNOXVILLE

Conclusions (Cont'd):

- As the aluminum content increases, the yield stress increases and plasticity ductility decreases.
- Al0.1CrCuFeMnNi shows good compression plasticity at 700°C and 800°C.
- Continue analyzing and modeling in-situ neutron levitation results.
- All binary and most of ternary systems have been thermodynamically modeled.

47

THE UNIVERSITY of TENNESSEE UT KNOXVILLE

BIG ORANGE BIG IDEAS

Thank You!

THE UNIVERSITY of TENNESSEE UT KNOXVILLE

Hot Compression Tests

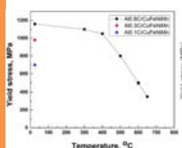

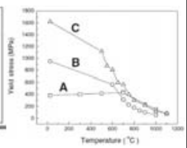

49

THE UNIVERSITY of TENNESSEE UT KNOXVILLE

Background and Unique Behavior (Cont'd)

Compression behavior at room temperature
BCC + FCC matrix, heat-treatment effect

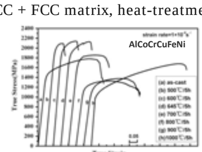

Compressive true stress–strain curves of AlCoCrCuFeNi after heat-treatment for 5 h at different temperatures.
The mechanical properties of this alloy have a strong correlation with the aging temperature.

L. H. Wen, H. C. Kou, J. S. Li, H. Chang, X. Y. Xue, and L. Zhou, Intermetallics 17, 266 (2009).

50

THE UNIVERSITY of TENNESSEE UT KNOXVILLE

Background and Unique Behavior (Cont'd)

The **AlxCrCuFeMnNi** system is good for high-temperature applications

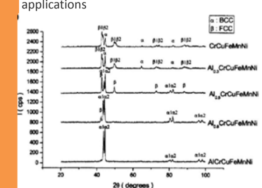

The AlxCrCuFeMnNi system is a mix of FCC and BCC phases.
Al = 0, 0.3
FCC1+FCC2+BCC
Al = 0.5, 0.8
FCC+BCC1+BCC2
Al = 1
BCC1 + BCC2

H. Y. Chen, C. W. Tsai, C. C. Tung, J. W. Yeh, T. T. Shun, C. C. Yang, and S. K. Chen, Annales De Chimie-Science Des Materiaux 31, 685 (2006).

51

THE UNIVERSITY of TENNESSEE UT KNOXVILLE

Preliminary Results - Alloy Fabrication

- Fabricate multiple alloy compositions belonging to the Al_xCrCuFeMnNi system varying the Al content from 0 to 2.
- Alloys sensitive to impurities and defects introduced during casting and processing
- Reduce defects during fabrication

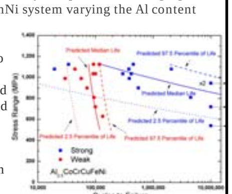

M. A. Hemphill, T. Yuan, G. Y. Wang, J. W. Yeh, C. W. Tsai, A. Chuang, and P. K. Liaw, Acta Materialia 60, 5723 (2012).

52

THE UNIVERSITY of TENNESSEE UT KNOXVILLE

PDF Studies at the SNS NOMAD

- Indications of a locally-strained crystal lattice

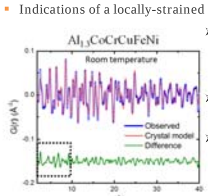

- The neutron-pair-distribution-function (PDF) data and the calculated PDF agree well at larger distances.
- As shown by the difference curve, the agreement below 10 angstrom is worse.
- This trend is consistent with the expectation that HEAs are locally strained, and yet, possess long-range crystal order.

L.J. Santodonato, Y. Zhang, M. Feygenson, C. Parish, J. Neuefeind, R.J.R. Weber, M.C. Gao, Z. Tang, and P.K. Liaw, (in review, 2014).

THE UNIVERSITY of TENNESSEE UT KNOXVILLE

PDF Studies at the SNS NOMAD

- Molten sample

At 1,400 °C, the observed PDF shows short-range order, consistent with a liquid phase, and agrees roughly with a model based upon local structures (less than 20Å diameters) composed B2 and FCC cells

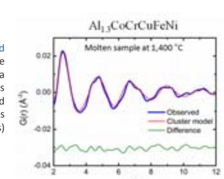

L.J. Santodonato, Y. Zhang, M. Feygenson, C. Parish, J. Neuefeind, R.J.R. Weber, M.C. Gao, Z. Tang, and P.K. Liaw, (in review, 2014).

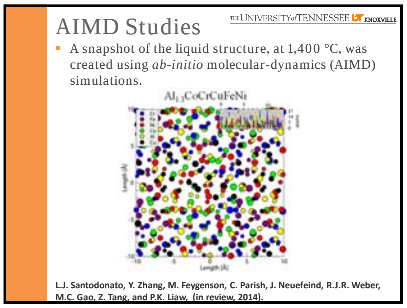
AIMD Studies
A snapshot of the liquid structure, at 1,400 °C, was created using ab-initio molecular-dynamics (AIMD) simulations.
Al1.3CoCrCuFeNi
L.J. Santodonato, Y. Zhang, M. Feygenson, C. Parish, J. Neuefeind, R.J.R. Weber, M.C. Gao, Z. Tang, and P.K. Liaw, (in review, 2014).

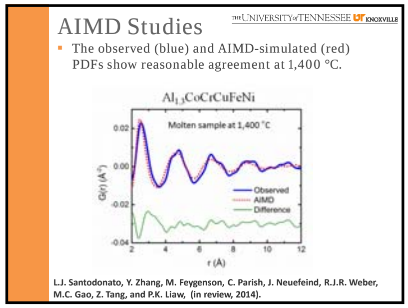
AIMD Studies
The observed (blue) and AIMD-simulated (red) PDFs show reasonable agreement at 1,400 °C.
Al1.3CoCrCuFeNi
Molten sample at 1,400 °C
Observed
AIMD
Difference
G(r) (Å⁻²)
r (Å)
L.J. Santodonato, Y. Zhang, M. Feygenson, C. Parish, J. Neuefeind, R.J.R. Weber, M.C. Gao, Z. Tang, and P.K. Liaw, (in review, 2014).

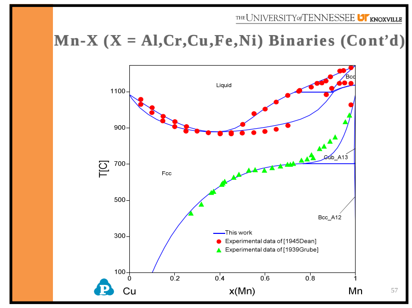
Mn-X (X = Al,Cr,Cu,Fe,Ni) Binaries (Cont'd)
Liquid
Fcc
Cub_A13
Bcc_A12
T[C]
This work
Experimental data of [1945Dean]
Experimental data of [1939Grube]
Cu
x(Mn)
Mn

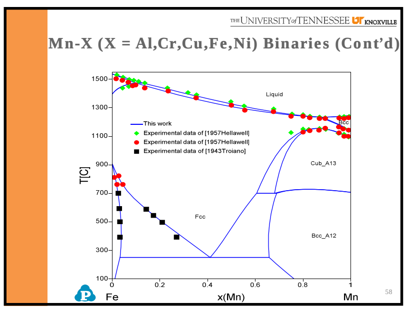
Mn-X (X = Al,Cr,Cu,Fe,Ni) Binaries (Cont'd)
Liquid
This work
Experimental data of [1957Hellawell]
Experimental data of [1957Hellawell]
Experimental data of [1943Troiano]
Cub_A13
Fcc
Bcc_A12
T[C]
Fe
x(Mn)
Mn

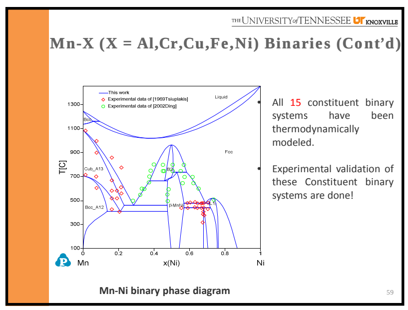
Mn-X (X = Al,Cr,Cu,Fe,Ni) Binaries (Cont'd)
All 15 constituent binary systems have been thermodynamically modeled.
Experimental validation of these Constituent binary systems are done!
T[C]
Mn
x(Ni)
Ni
Mn-Ni binary phase diagram

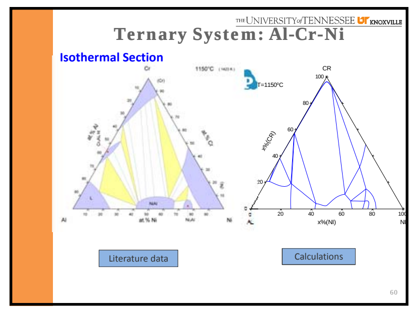
Ternary System: Al-Cr-Ni
Isothermal Section
T=1150°C
Literature data
Calculations

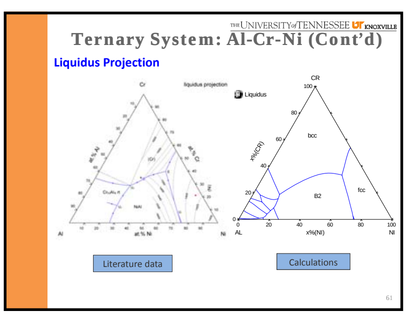
Ternary System: Al-Cr-Ni (Cont'd)
Liquidus Projection
Liquidus
bcc
B2
fcc
Literature data
Calculations

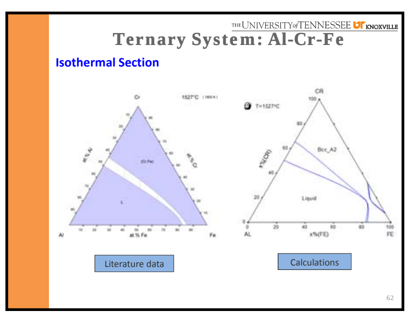
Ternary System: Al-Cr-Fe
Isothermal Section
T=1527°C
Bcc_A2
Liquid
Literature data
Calculations

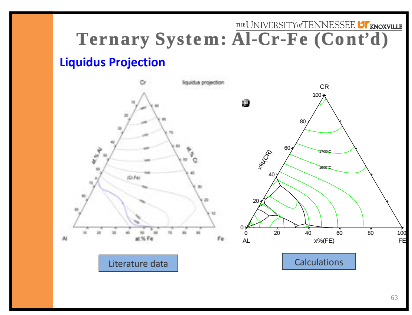
Ternary System: Al-Cr-Fe (Cont'd)
Liquidus Projection
Literature data
Calculations

Ternary System: Al-Cr-Fe (Cont'd)

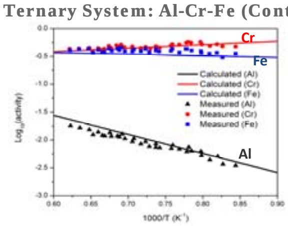

Comparison of the calculated and measured thermodynamic activities of Al, Cr, and Fe in the alloy with target composition of Fe-19.9Al-30.2Cr (at.%)

Al-Fe-Mn Ternary System

Isothermal section at 800°C

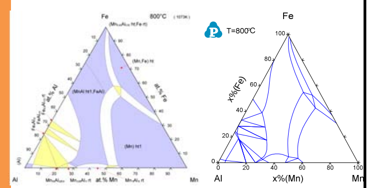

Literature data — Calculation of this work

Al-Fe-Mn Ternary System (Cont'd)

Liquidus projection

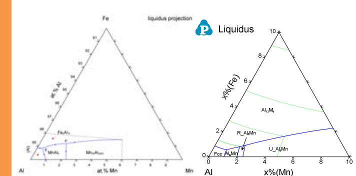

Literature data — Calculation of this work

Al-Cu-Ni Ternary System

Isothermal section at 500°C

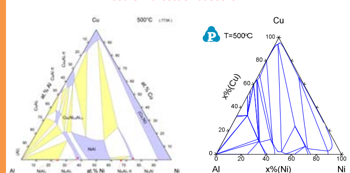

Literature data — Calculation of this work

Al-Cu-Ni Ternary System (Cont'd)

Liquidus projection

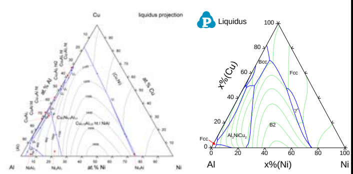

Literature data — Calculation of this work

Alloy System

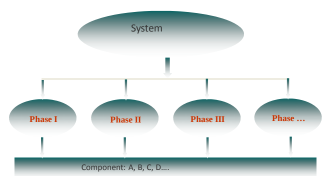

$$G_m^p = f(x_i; T; parameters)$$

Simple Binary System: Ti-V

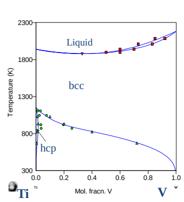

Liquid, bcc, hcp:

disordered solution phases

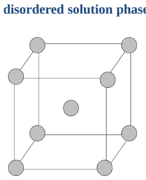

Gibbs Energy Function of Substitutional Solution Model

$$G = x_A \cdot G_A^{o,\varphi} + x_B \cdot G_B^{o,\varphi} + RT \cdot (x_A \ln x_A + x_B \ln x_B) + G^{ex}$$

x_A, x_B --- mole fractions of component A and B.

$G_A^{o,\varphi}, G_B^{o,\varphi}$ --- Gibbs energy of pure A, and B with φ structure.

R --- Gas constant.

T --- Temperature.

$$G^{ex} = x_A \cdot x_B \cdot \sum_{i=0}^{n} \lambda_i \cdot (x_A - x_B)^i$$

λ_i – Model parameters, obtained by optimization using available experimental data

Regular solution model: $G^{ex} = \lambda_0 \cdot x_A \cdot x_B$

Complicated Binary System: Ni-Al

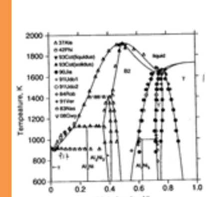

Disordered solution phases:

Liquid, fcc (γ)

Stoichiometric phases:

Al_3Ni, Al_3Ni_5

Ordered intermetallic phases:

Al_3Ni_2, B2, γ′

Other Model Types (I)

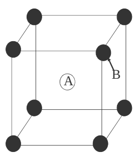

•Stoichiometric Phase:

$$G = x_A G_A^{o,\phi} + x_B G_B^{o,\phi} + \Delta G_f$$

$$\Delta G_f = a + b\cdot T + c\cdot T\cdot \ln T + \cdots$$

$a, b, c, \cdots$: parameters

THE UNIVERSITY of TENNESSEE UT KNOXVILLE

Other Model Types (II)

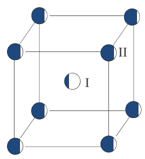

Ordered Intermetallic Phase:

$$y_P^i$$

$$\sum_{P=A,B} y_P^i = 1 \quad (y_A^I + y_B^I = 1)$$

$$G = G(x, y, T, parameters)$$

THE UNIVERSITY of TENNESSEE UT KNOXVILLE

Other Model Types (II)

$$G_m^{\varphi} = \sum_{i=A,B}\sum_{j=A,B} y_i^I y_j^{II} G_{i:j}^{\varphi} + RT[\frac{p}{p+q}\sum_{i=A,B} y_i^I \ln y_i^I + \frac{q}{p+q}\sum_{i=A,B} y_i^{II} \ln y_i^{II}] + \sum_{j=A,B} y_A^I y_B^I y_j^{II} \sum_v (y_A^I - y_B^I)^v L_{A,B:j}^v + \sum_{i=A,B} y_i^I y_A^{II} y_B^{II} \sum_v (y_A^{II} - y_B^{II})^v L_{i:A,B}^v + y_A^I y_B^I y_A^{II} y_B^{II} L_{A,B:A,B}$$

Compression Tests

THE UNIVERSITY of TENNESSEE UT KNOXVILLE

		2×10^{-3} s^{-1}	2×10^{-4} s^{-1}	5×10^{-5} s^{-1}
$Al_{0.1}CrCuFeMnNi$	n	0.41	0.37	0.36
	K (MPa)	498	567	584
$Al_{0.3}CrCuFeMnNi$	n	0.40	0.34	0.44
	K (MPa)	596	633	550
$Al_{0.8}CrCuFeMnNi$	n	0.23	0.22	0.24
	K (MPa)	1043	1054	1043

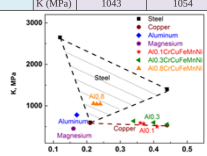

Callister, Jr., William D (2005), Fundamentals of Materials Science and Engineering (2nd ed.), pp: 152.

76

THE UNIVERSITY of TENNESSEE UT KNOXVILLE

Background and Unique Behavior (Cont'd)

The **AlxCrCuFeMnNi** system is good for high-temperature applications

The **AlxCrCuFeMnNi** has greater hardness values than its counterpart, **AlxCrCuFeCoNi**

Mn :BCC stabilizer ➡ increased hardness.

The chromium-high manganese austenitic stainless **steels** work hardens more than Type 304 steel. This phenomenon is due to the **deformation-induced austenite-to-martensite transformation** and **twinning-induced plasticity (TWIP) effect**.

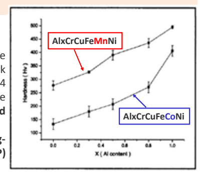

H. Y. Chen, C. W. Tsai, C. C. Tung, J. W. Yeh, T. T. Shun, C. C. Yang, and S. K. Chen, Anna De Chimie-Science Des Materiaux 31, 685 (2006).

77

THE UNIVERSITY of TENNESSEE UT KNOXVILLE

In-situ neutron-diffraction

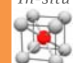

- small-contrast B2 sample (Al1.3CoCrCuFeNi)
- high-contrast B2 sample (Al1.3MnCrCuFeNi)

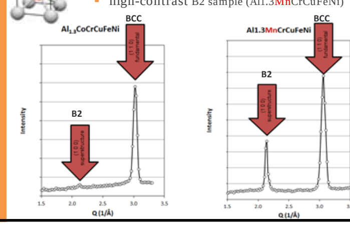

THE UNIVERSITY of TENNESSEE UT KNOXVILLE

Results-Nanoindentation (Al0.8CrCuFeMnNi-HIP-899°C)

Load-displacement curves of the Al0.8CrCuFeMnNi at different indentation loading rates

4-sided pyramid indenter

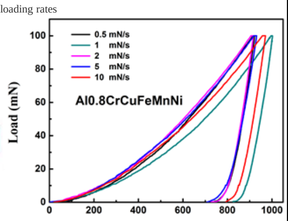

THE UNIVERSITY of TENNESSEE UT KNOXVILLE

Ab-initio Molecular-dynamics (AIMD) Studies

- Selected partial-pair-correlation functions, $g_{ab}(r)$, indicate that some pairs (e.g., Al-Ni, Cr-Fe, and Cu-Cu) are much more likely to be found as nearest neighbors than others (e.g., Al-Al and Cr-Ni).
- Such preferred nearest-neighbor pairing in the liquid phase is consistent with the formation of a B2-ordered solid-solution primary phase, which is supported by the presence of superstructure peaks in the high-temperature diffraction data

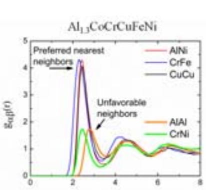

L.J. Santodonato, Y. Zhang, M. Feygenson, C. Parish, J. Neuefeind, R.J.R. Weber, M.C. Gao, Z. Tang, and P.K. Liaw (in review, 2014).

Compression Tests

THE UNIVERSITY of TENNESSEE UT KNOXVILLE

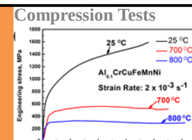

As the aluminum content increases,
- ❑ Yield stress increases
- ❑ Compression plasticity decreases

This phenomenon is due to the increased strengthening effect of lattice strains caused by the lattice-sites occupation of Al.

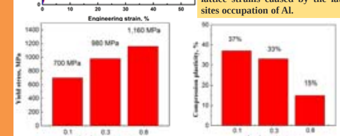

Z. Tang, M. C. Gao, H. Diao, T. Yang, J. Liu, T. Zuo, Y. Zhang, Z. Lu, Y. Cheng, Y. Zhang, K. A. Dahmen, P. K. Liaw, and T. Egami, JOM, 65, 12 (2013).

81

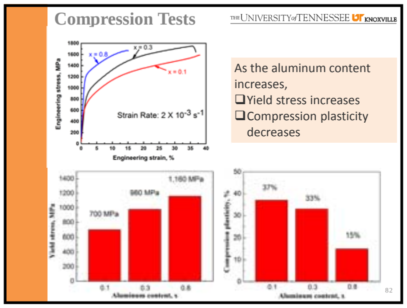
Compression Tests
THE UNIVERSITY of TENNESSEE UT KNOXVILLE
x = 0.8
x = 0.3
x = 0.1
Strain Rate: 2 X 10-3 s-1
Engineering stress, MPa
Engineering strain, %
As the aluminum content increases,
Yield stress increases
Compression plasticity decreases
700 MPa
960 MPa
1,160 MPa
Yield stress, MPa
Aluminum content, x
37%
33%
15%
Compression plasticity, %
Aluminum content, x
82